Journal Pre-Proof

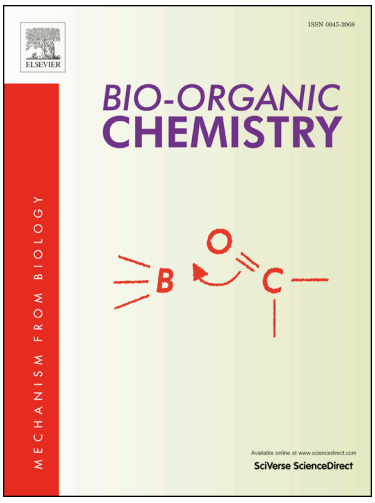

Synthesis of novel (*R*)-4-fluorophenyl-1*H*-1,2,3-triazoles: A new class of α-glucosidase inhibitors

Satya Kumar Avula, Ajmal Khan, Sobia Ahsan Halim, Zahra Al-Abri, Muhammad U. Anwar, Ahmed Al-Rawahi, Rene Csuk, Ahmed Al-Harrasi

PII: S0045-2068(19)30452-3
DOI: https://doi.org/10.1016/j.bioorg.2019.103182
Reference: YBIOO 103182

To appear in: *Bioorganic Chemistry*

Received Date: 22 March 2019
Revised Date: 4 July 2019
Accepted Date: 1 August 2019

Please cite this article as: S. Kumar Avula, A. Khan, S. Ahsan Halim, Z. Al-Abri, M.U. Anwar, A. Al-Rawahi, R. Csuk, A. Al-Harrasi, Synthesis of novel (*R*)-4-fluorophenyl-1*H*-1,2,3-triazoles: A new class of α-glucosidase inhibitors, *Bioorganic Chemistry* (2019), doi: https://doi.org/10.1016/j.bioorg.2019.103182

Synthesis of novel (*R*)-4-fluorophenyl-1*H*-1,2,3-triazoles: A new class of α-glucosidase inhibitors

Satya Kumar Avula[a], Ajmal Khan[a], Sobia Ahsan Halim[a], Zahra Al-Abri[a], Muhammad U. Anwar[a], Ahmed Al-Rawahi[a], Rene Csuk[b], Ahmed Al-Harrasi[a*]

[a]*Natural and Medical Sciences Research Center, University of Nizwa, P.O. Box 33, Postal Code 616, Birkat Al Mauz, Nizwa, Sultanate of Oman (phone: +968 25446328; e-mails: aharrasi@unizwa.edu.om)*

[b]*Organic Chemistry, Martin-Luther-University Halle-Wittenberg, Kurt-Mothes-Str. 2, d-06120, Halle (Saale), Germany*

***Corresponding author (A. Al-Harrasi)**

[a]Natural and Medical Sciences Research Center, University of Nizwa, P.O. Box 33, Postal Code 616, Birkat Al Mauz, Nizwa, Sultanate of Oman (phone: +968 25446328; e-mails: aharrasi@unizwa.edu.om)

Abstract: Diabetes is a non-communicable disease, which occurs either due to the lack of insulin or the inability of the human body to recognize it. The recent data indicates an increase in the trend of people diagnosed with Type 2 diabetes mellitus (T2DM). *α*-Glucosidase inhibitors are known to reduce the impact of carbohydrates on blood glucose level and prevent the digestion of carbohydrates. *α*-glucosidase inhibitors hold great potential for the treatment of T2DM. In search of better *α*-glucosidase inhibitors, a series of novel (*R*)-4-fluorophenyl-1*H*-1,2,3-triazole derivatives were synthesized (**6 and 8a-n**) and evaluated for their *α*-glucosidase inhibitory activity *in vitro*. All new compounds were characterized by ^{1}H NMR, ^{13}C NMR, ^{19}F NMR, ESI-MS, and where applicable by single crystal X-ray diffraction (**8m**). A preliminary structure-activity relationship suggested that the presence of 1*H*-1,2,3-triazole ring in (*R*)-4-fluorophenyl-1*H*-1,2,3-triazole derivatives has remarkable contribution in the overall activity. Molecular docking studies were carried out to investigate the binding mode of compounds within the active site of the *α*-glucosidase enzyme. Docking results are in complete agreement with the experimental finding. This study unravelled a new class of triazole derivatives with *α*-glucosidase inhibitory activity.

Keywords: Synthesis, (*R*)-4-fluorophenyl-1*H*-1,2,3-triazoles, X-ray crystallography, *α*-Glucosidase inhibitor, Molecular docking studies.

1. Introduction

Nitrogen containing heterocyclic compounds play a vital role in the pharmaceuticals and agrochemicals [1].

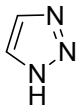

1*H*-1,2,3-triazole

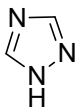

1*H*-1,2,4-triazole

Among the heterocyclic systems in organic chemistry, 1,2,3-triazoles hold great importance due to their broad spectrum of applications in pharmaceuticals, biochemical, medicinal and material sciences [2]. Their chemistry underwent a substantial growth over the past decades [3,4]. 1*H*-1,2,3-triazole containing compounds were reported to exhibit a large range of biological activities such as antimicrobial activity against gram positive bacteria [5], anti-HIV [6,7], antiviral [8], antiallergic [9], antifungal [10,11], anticonvulsant [12] and anti-nociceptive activity [13]. Moreover, these derivatives were also utilized as intermediates for the synthesis of antibiotics [14,15], fungicides [16], insecticide [17] and, plant growth regulators [18]. They are widely used in industrial applications such as photo stabilizers, dyes, photographic materials, corrosion inhibition (of copper and copper alloys), and agrochemicals [19]. The fluorine containing 1,2,3-triazole derivatives could be a subject of special interest. Incorporation of fluorine atom is known to significantly influence the physical and chemico-biological properties of the organic molecules [20,21]. Due to this, great efforts have been exerted to develop new synthetic methodologies toward fluorine-containing moieties in particular fluorinated heterocycles. In contrast, a limited number of fluoro-substituted 1,2,3-triazoles have been reported [22,23]. Rufinamide is commercially available drug which contain 1*H*-1,2,3-triazole (Fig. 1). It blocks calcium channels, a severe form of childhood epilepsy and it has been approved for the treatment of *Lennox-Gastaut* syndrome [24].

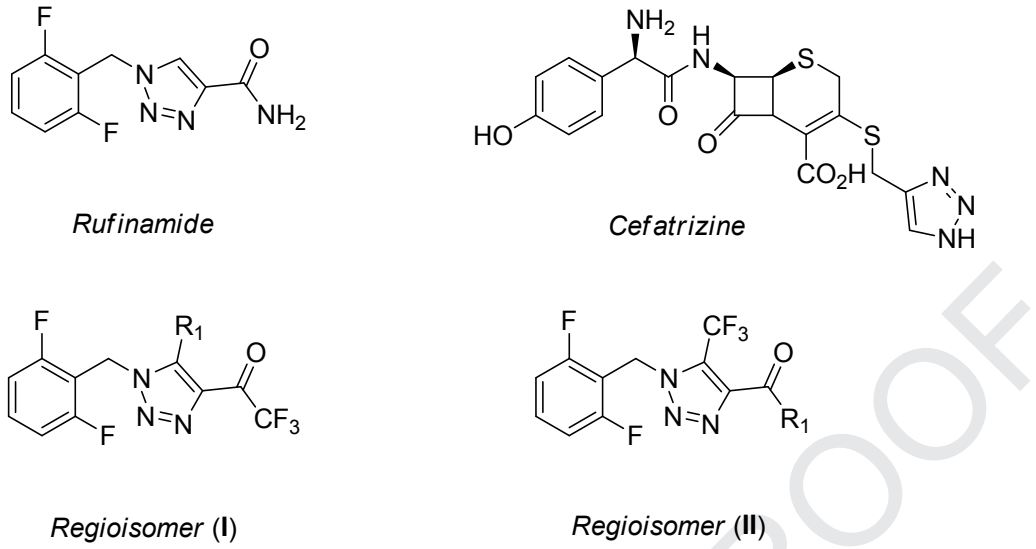

Fig. 1. Chemical Structures of some bioactive 1*H*-1,2,3-triazole derivatives

α-Glucosidase is a potential drug target for type 2 Diabetes mellitus (T2DM) [25, 26], which is one of the most common and serious metabolic diseases characterized by high blood-glucose levels [27]. T2DM is mainly treated by the inhibition of carbohydrate hydrolysing enzymes which in turn suppress the postprandial hyperglycemia by reducing the absorption of gut glucose [28]. Thus, the inhibition of α-glucosidase to control elevated glucose levels in blood is a popular choice [29]. *α*-Glucosidase inhibitors (AGIs) including acarbose, miglitol and voglibose, are associated with side effect like flatulence, diarrhea and abdominal discomfort and have low efficacy with high IC_{50} values [30]. Recent studies have demonstrated that 1,2,3-triazole ring containing heterocycles are superior *α*-glucosidase inhibitors (Fig. 2) [31].

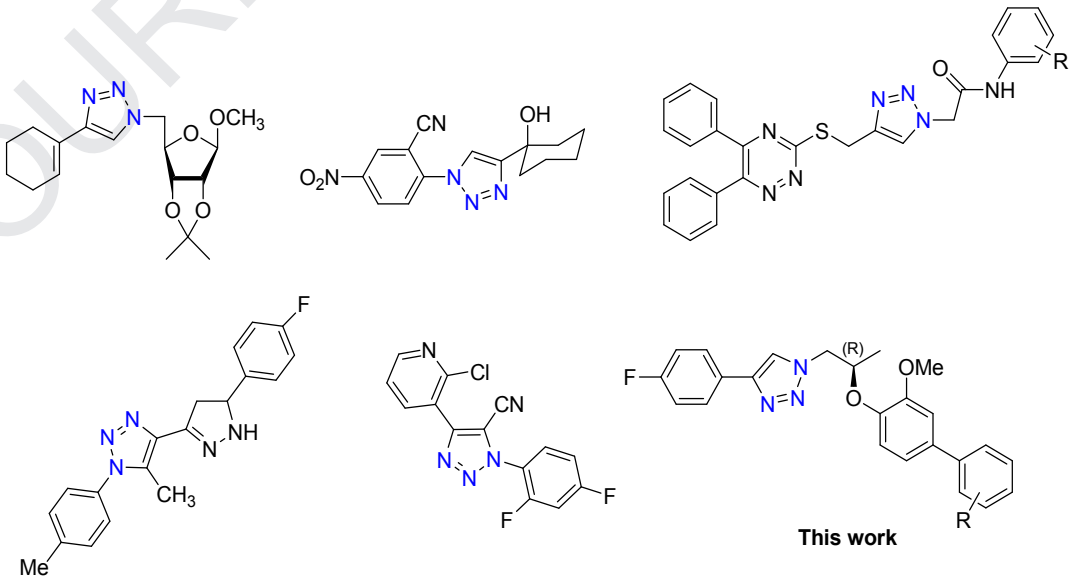

Fig. 2. Chemical Structures of some 1*H*-1,2,3-triazole derivatives as potential *α*-glucosidase inhibitors.

Our recent report in this series suggest its potential α-glucosidase inhibitory activity [32]. In continuation to our previous findings [32,33], we herein report the synthesis and *in vitro* anti-α-glucosidase activity of a new series of fluorine containing (*R*)-4-fluorophenyl-1*H*-1,2,3-triazole derivatives. Furthermore, structural-activity relationship as well as molecular docking results are thoroughly discussed.

2. Results and discussion

2.1. Chemistry

*2.2. Synthesis of (R)-4-fluorophenyl-1H-1,2,3-triazole bromide (**6**)*

The key intermediate (*R*)-4-fluorophenyl-1*H*-1,2,3-triazole bromide **6** was synthesized using a convenient five-step procedure starting from the commercially available (*S*)-ethyl lactate **1** *via* modified chiron approach as shown in Scheme 1 [32]. The ^{1}H NMR spectrum of compound **6** showed a doublet at δ 1.31 which is attributed to methyl protons of –CH–O–Ph and a singlet peak at δ 3.74, which is assigned to methoxy protons on phenyl ring. A doublet of doublet (δ = 4.54) and a multiplet (δ = 4.64) signals correspond to the –CH–O– and –CH_2–N–, respectively. The seven aromatic protons appeared in the region of δ 7.76-6.68 ppm, while a singlet appeared at δ 8.02 for triazole proton (–CH–N_3). The structure of compound **6** was confirmed by 2D NMR experiments (HMBC, HSQC, COSY and NOESY) as well. The high-resolution mass spectrometric (HRMS) data at 406.0567 (M+H) further supports the reported structure.

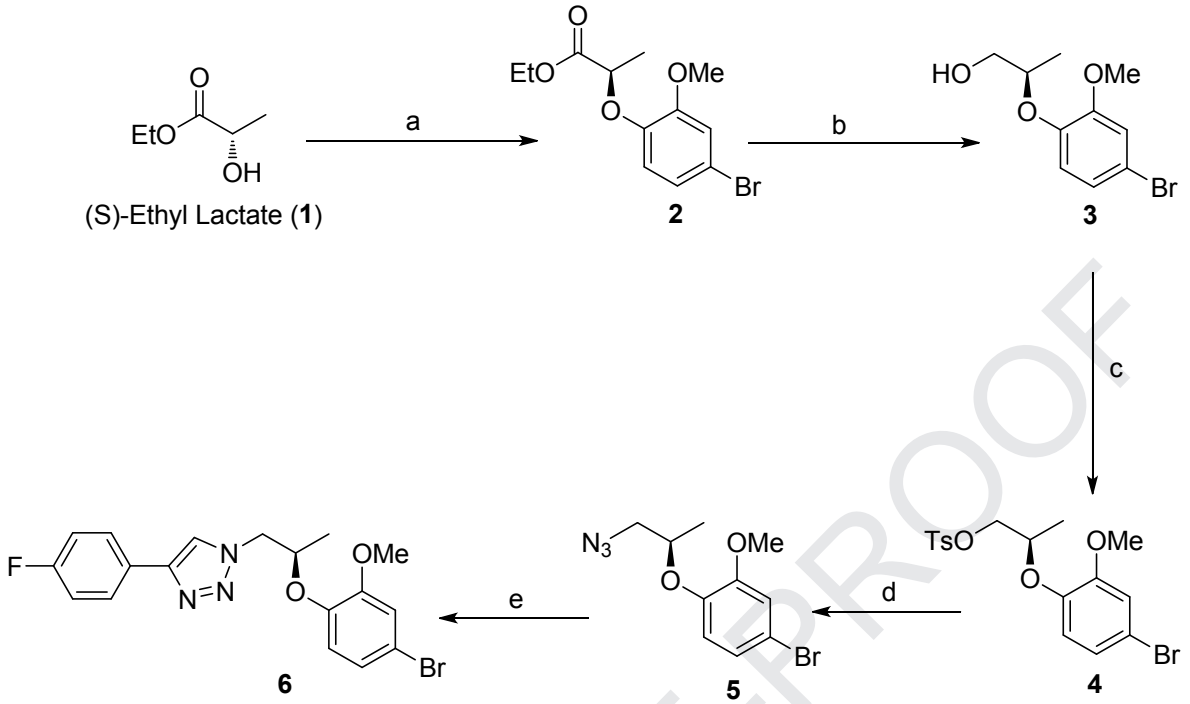

Scheme 1. Reagents and conditions: (a) 4-bromo-2-methoxyphenol, PPh_3, DIAD, dry THF, 0 °C to room temperature, 3 h, 86%; (b) DIBAL-H, dry DCM, 0 °C to room temperature, 3 h, 90%; (c) TsCl, Et_3N, dry DCM, DMAP, 0 °C to room temperature, 5 h, 95%; (d) NaN_3, DMF, 70 °C, 3 h, 78%; (e) 1-ethynyl-4-fluorobenzene, CuI, Et_3N, CH_3CN, room temperature, 3 h, 79%.

*2.3. Synthesis of (R)-4-fluorophenyl-1H-1,2,3-triazole derivatives (**8a-n**)*

The final step was functionalization of the aryl bromide moiety by Suzuki-Miyaura reaction [34,35] of (*R*)-4-fluorophenyl-1*H*-1,2,3-triazole bromide **6** with different arylboronic acids **7a-n** (1.5 equiv) afforded the (*R*)-4-fluorophenyl-1*H*-1,2,3-triazole derivatives **8a-n** in 69-86% yields (Scheme 2, Table 1). Both electron-poor and electron-rich arylboronic acids were successfully employed. The reactions were clean and the best yields were obtained in 1, 4-dioxane at 120 °C using Pd $(PPh_3)_4$ (5 mol %) as a catalyst and K_2CO_3 (3.0 equiv) as a base.

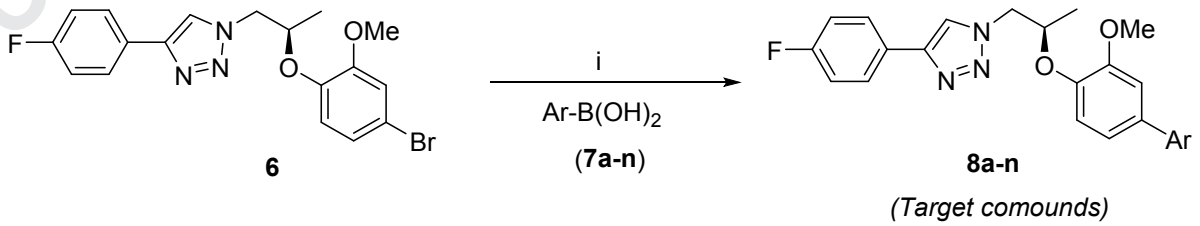

Scheme 2. Synthesis of Target compounds (**8a-n**). Reagents and conditions: (i) **6** (1.0 equiv), **7a-n** (1.5 equiv), Pd $(PPh_3)_4$ (5 mol %), K_2CO_3 (3.0 equiv), 1, 4-dioxane, 120 °C, 8 h.

Table 1: Synthesis of (*R*)-4-fluorophenyl-1*H*-1,2,3-triazole derivatives (**8a-n**).

Reagents (7)	Compounds (8)	Ar[1]	Yield of 10 (%)[a]
a	**a**	Ph	76
b	**b**	4-MeC_6H_4	73
c	**c**	4-MeOC_6H_4	69
d	**d**	4-$NO_2C_6H_4$	85
e	**e**	4-ClC_6H_4	82
f	**f**	4-NCC_6H_4	79
g	**g**	4-FC_6H_4	84
h	**h**	3,5-$(F_3C)_2C_6H_3$	80
i	**i**	4-CHOC_6H_4	77
j	**j**	2,6-$(F)_2C_6H_3$	82
k	**k**	2,3,4-$(F)_3C_6H_2$	86
l	**l**	2-$C_{10}H_7$	79
m	**m**	4-AcC_6H_4	82
n	**n**	2-C_8H_5S	78

[a]Yields refer to pure isolated products.

The chemical structures of the (*R*)-4-fluorophenyl-1*H*-1,2,3-triazole derivatives (**8a-n,** target compounds) were confirmed by spectroscopic techniques (^{1}H NMR, ^{13}C NMR, ^{19}F NMR, IR and HRMS). Single crystals of **8m** were grown from slow evaporation CH_2Cl_2 solution. The structure of compound **8m** was unambiguously confirmed by X-ray crystal structure analysis (Fig. 3).

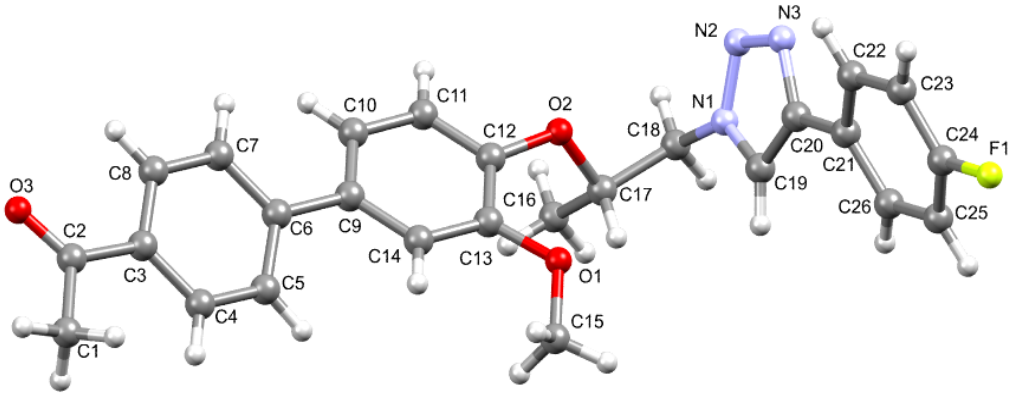

Fig. 3. Crystal structure of compound **8m**

Biological activity

Screening of all compounds suggested significant inhibition of α-glucosidase by all compounds with IC_{50} values in range of 17.9±0.4 - 193.7±0.42 μM (Table-2), when compared to the standard drug acarbose (IC_{50} = 942 ± 0.74 μM). Incorporation of unsubstituted phenyl ring at Ar position, decreased the activity of *1H*-1,2,3-triazole derivatives observed in compound **8a** (IC_{50} = 193.7±0.42 μM). On the other hand, addition of a methyl group on this phenyl is responsible to activate the ring, as a result activity was increased as seen in compound **8b** (IC_{50} = 84.2±2.6 μM). The activity of this series was further enhanced by adding a stronger electron donating group as observed in compound **8c** having methoxy group which resulted in IC_{50} value of 66.8±1.2 μM. A similar trend was observed for compounds **8d-8j**. The activity of this series was further improved when more functionalities were introduced (compounds **8k-8n)**. The detailed structure-activity relationship was explained in the molecular docking studies.

Table 2: α-Glucosidase inhibitory activities, molecular docking scores and molecular interactions of compounds **8a-8n**

Compounds	IC_{50} ± SEM (μM)	Docking Score	Interactions (Å)
8a	193.7±0.42	-4.39	O11---Wat1174 (1.77) O48---Wat1056 (2.05)
8b	84.2±2.6	-4.44	N25---Asn241 (2.67)
8c	66.8±1.2	-4.86	O11---Wat1174 (1.71) O47---Wat1056 (1.92)
8d	59.5±1.1	-4.90	O48---His111 (2.81)
8e	48.6±0.8	-5.73	O11---Wat1174 (1.77) O48---Wat1056 (1.88)
8f	43.7±0.8	-5.91	N25---Asn241 (2.81)
8g	37.6±0.45	-6.36	O11---Wat1174 (1.80)
8h	40.18±0.6	-6.27	F53---Arg439 (2.74) Triazole ring---His 279 (π-π)
8i	57±3.4	-5.67	O54---His111 (1.83)
8j	44.3±0.6	-5.74	O11---Wat1174 (1.79) O48---Wat1056 (2.34)
8k	21.7±0.8	-7.18	O11---Wat1174 (1.78) N25---Asn241 (3.12) F53---Arg212 (3.10) F55---His348 (2.47)

8l	17.9±0.4	-7.41	O11---Wat1174 (1.65) N25---Asn241 (2.45)
8m	29.5±0.26	-6.48	O52---Wat1026 (2.35) Triazole-ring---His279 (π-π) N25---Asn241 (2.66)
8n	23.9±1.1	-6.89	S38---Wat1102 (2.17) S38---Asp349 (3.21) N25---Asn241 (2.63)
Acarbose (Standard)	942 ± 0.74	-3.90	O15---Glu304 (2.68) O17---Pro309 (2.82) N37--- Glu304 (3.54) O64---Wat1102 (2.73) O79---Glu276 (2.54) O81---Asp349 (2.84) O44---Wat1174 (2.70) O81---Arg212 (3.07) O83--- His348 (3.33) O83---Wat1026 (2.92) O87--- His111 (2.81) N37--- Glu304 (3.54)

SEM= Standrad error mean

Molecular molding and docking analysis

For docking, homology modelling was conducted to predict the three dimensional (3D) structure of *Saccharomyces cerevisiae*. α-Glucosidase enzyme, and its properties were evaluated to check the quality of the model. The protein is composed of total 579 residues. The Ramachandran plot showed that 444 (86.7%), 63 (12.3%), 3 (0.6%), and two (0.4%) residues lied in the most favored, additional allowed, generously allowed, and disallowed regions, respectively. However, two residues (Ala278 and Thr566), which are displayed in disallowed region are not a part of active site region. ERRAT showed 93.52 quality factor and Verify3D depicted that 95.5% residues showed average 3D-1D score of 0.7. The model is of good quality. The active site residues were predicted by superimposing the closest homologue (72% identity) i.e. *S. cerevisiae.* Isomaltase enzyme in complex with isomaltose (PDB code: 3AXH) which suggests that Asp214 and Glu276 of *S. cerevisiae* α-glucosidase act as nucleophile and proton donor, respectively. While Asp349 act as a transition state

stabilizer for substrate molecule. The catalytic site is composed of Asp214, Glu276, and Asp349. While several residues including Asp68, Tyr71, Val108, His111, Phe157, Phe158, Phe177, Gln181, Arg212, Thr215, Leu218, Glu276, Ala278, Phe300, Arg312, His348, Asp349, Gln350, Asp408, Arg439, Arg443 surround the catalytic site. Moreover some water molecules including Wat1021, Wat1026, Wat1056, Wat1058, Wat1061, Wat1087, Wat1102, Wat1122, Wat1174, and Wat1228 plays crucial role in the binding of the substrate molecule. The entrance of the active site is composed of Phe231, His239, Asn241, His279, Glu304, and Arg312. Phe231, and His239 act as a gate keeper residues that opens when ligand comes inside the gorge. The overall topology of the model is presented in Figure 4.

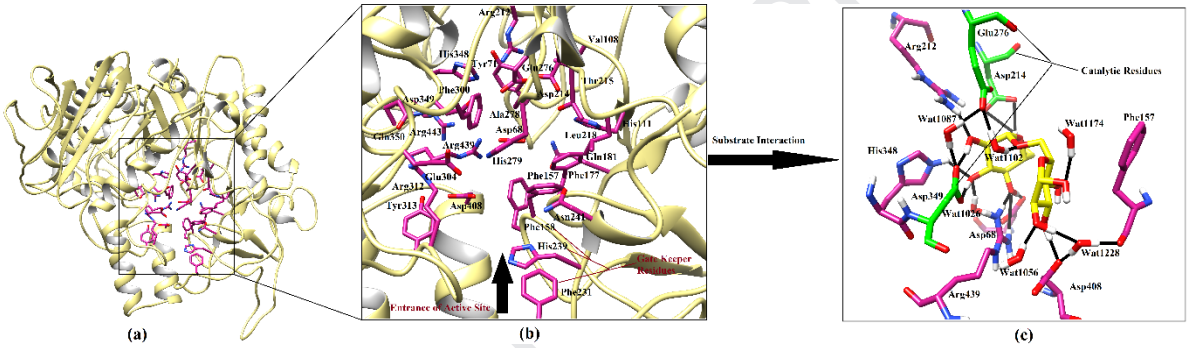

Figure 4: (a) The three-dimensional structure of protein model. (b). The active site is highlighted in box. Residues are depicted in pink stick, while protein is shown in gold helix. (c). Interactions of substrate molecule (isomaltose) with the active site residues and water molecules is shown. Substrate moiety is depicted in yellow stick, the catalytic residues are shown in green sticks, and hydrogen bonds are shown in black lines.

Structure-activity relationship

All the compounds (**8a-8n**) along with the standard compound (acarbose) were docked into the active site of *S. cerevisiae* α-Glucosidase. All the compounds adopted similar orientation, fluorophenyl substituted triazole moiety interacts at the entrance of the active site, while the substituted biphenyl moiety is oriented towards the catalytic residues. The triazole moiety of the most active compound **8l** forms hydrogen bond with the side chain carboxamide nitrogen of Asn241, while phenyl oxygen accepts hydrogen bond from the surrounding water molecule (Wat1174). The docking results show that water molecules in the active site are important in stabilizing the protein ligand interactions. Moreover the side chains of His111,

Phe177 and Tyr71 provides π-π interactions to the naphthalene ring of the compound. Compounds **8k**, **8n**, and **8m** displayed activities in range of 21-29μM. The docked view of these compounds demonstrated that the electronegative group at biphenyl ring is responsible for the binding of these compound with the side chains of Arg212, His348, Asp349, and His279. These residues are lied at the base of the gorge, thus these interactions stabilize the compounds in the active site. In addition, substitution of the bulky groups at this position is responsible for the decreased activity of the compound. For instance, compounds **8g**, **8h**, **8f**, **8j** and **8e** exhibited activities in range of 37-48μM. These compounds may either loss water mediated bridging or bonding with the side chain of Asn241, as a result their activities are reduced. Compounds **8i**, **8d**, **8c**, and **8b** depicted activities in range of 59-84μM. The aldehydic oxygen of compound **8i** mediates hydrogen bonding with the side chain of His111, however this compound does not bind with the water molecules or Asn241. Similarly, nitrite oxygen of compound **8d** forms hydrogen bond with the side chain of His111. The methoxy oxygen of compound **8c** interacts with water molecules but do not interact with Asn241, or His111. The binding mode of compound **8b** suggests that this compound interacts with the Asn241, while it doesn't mediate any interactions with the water molecule or the residues lied at the base of active site. The least active compound (**8a**) does not interact with Asn241, instead it's triazole moiety is tilted more towards Arg312, however triazole moiety does not form bond with Arg312. Methoxy oxygen and biphenyl substituted oxygen may interact with the water molecules. The docking results revealed an important role of Asn241, it's side chain carboxamide group acts as a hydrogen bond donor to the triazole nitrogen of active compounds. Moreover, two water molecules Wat1056, and Wat1174 plays crucial role in protein-ligand bridging. Water molecule 1056 forms bidentate interaction with the side chain guanidinium moiety of Arg312, thus this water molecule bridges the ligand with the side chain of Arg312. Water molecule 1174 does not interact with the surrounding residues, however it has interactions with the ligands. Compounds **8m** and **8n** interact with water molecules 1026 and 1102, respectively. Wat1026 bridges ligand **8m** with the side chain of Asp68, while 1102 bridges **8n** with the side chain of the catalytic residue Glu276, thus these water mediated bridging helps to stabilize the interactions of ligands with in the active site. The interaction of each ligand and their docking scores are tabulated in Table 2. The docking results are in complete agreement with the experimental findings and the docking score correlates well with the inhibitory potency of compounds. The docked poses of all the compounds are shown in Figure 5.

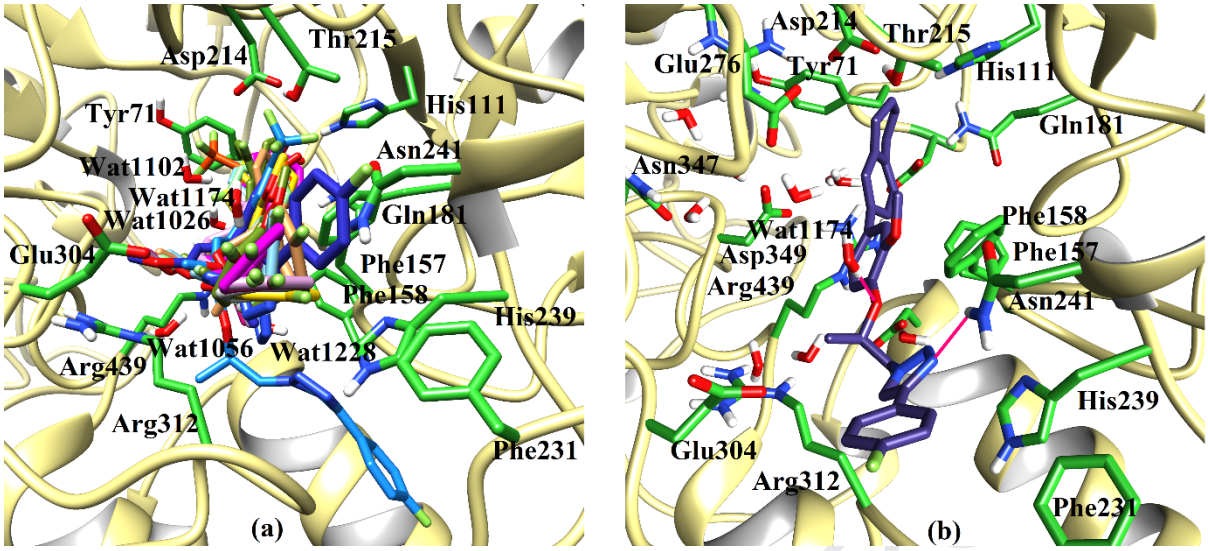

Figure 5: (a). The binding orientation of Compounds **8a-8n** in the active site of *S. cerevisiae* α-glucosidase (b). The docked view of most active compound **8l** is presented. Compounds is shown in purple sticks, active side residues are shown in green sticks, while hydrogen bonds are depicted in pink lines.

3. Conclusions

In summary, a series of (*R*)-4-fluorophenyl-1*H*-1,2,3-triazole derivatives (**8a-8n**) were designed, synthesized and evaluated as novel *α*-glucosidase inhibitors. Therefore, a fluoro group was the most favourable substituent on the phenyl ring and 1,2,3-triazole ring in (*R*)-4-fluorophenyl-1*H*-1,2,3-triazole derivatives are responsible for the anti-*α*-glucosidase activity. Further studies on the structural optimization of these derivatives are still underway in our laboratory.

4. Experimental Section

4.1. General

All experiments were carried out in dry reaction vessels under dry nitrogen atmosphere. All reagents were purchased from Sigma-Aldrich chemical company, Germany. Solvents were purified and dried by standard procedures before use in experiments. The spectra were recorded with the following instruments; IR: PerkineElmer RX FT-IR spectrophotometer; IR wave numbers (ν) are given in cm^{-1}. HR-ESI-MS: Agilent Technologies, 6530 Accurate Mass. The ^{1}H- and ^{13}C-NMR spectra were recorded on 600 MHz and 150 MHz spectrometers using the solvent peak as internal reference ($CDCl_3$, δ H: 7.26; δ C: 77.0). The ^{19}F-NMR

spectra was recorded on 564 MHz spectrometer. Data were reported in the following order: chemical shift (δ) in ppm; multiplicities are indicated: m = multiplet; q = quadrate, dd = doublet of doublet, t = triplet, d = doublet, s = singlet; coupling constants (*J*) are in hertz (Hz). HPLC technique was performed with variable wavelength detector. Column chromatography was carried out by using silica gel of the selected particle size of 100-200 mesh. All reactions were monitored by Thin-Layer-Chromatography (TLC) using silica gel F_{254}. Visualization was accomplished with UV-light and I_2 stain. Solvents for the catalytic reaction were technical grade and dried by standard procedures. Solvents for column chromatography (EtOAc, *n*-hexane) were technical grade and distilled prior to use. Organic extracts were dried over anhydrous Na_2SO_4). For X-ray measurements, single crystal of **8m** was mounted on a MiTeGen loop with grease and examined on a Bruker D8 Venture APEX diffractometer equipped with Photon 100 CCD area detector at 296 (2) K using graphite-monochromated Mo-Kα radiation (λ = 0.71073Å). Data was collected using the APEX-II software [36], integrated using SAINT [37], and corrected for absorption using a multi-scan approach (SADABS) [38]. The structure was solved using intrinsic phasing (SHELXT) [39]. Final cell constants were determined from full least squares refinement of all observed reflections. All non-H atoms were located in subsequent difference maps and refined anisotropically with SHELXL-97 [40], using full least squares refinement against F2. H-atoms were added at calculated positions and refined with a riding model. The structure has been deposited with the CCDC (CSD deposition numbers 1903648).

*4.2. General procedure for preparation of (R)-4-fluorophenyl-1H-1,2,3-triazole bromide (**6**).*

The key intermediate (*R*)-4-fluorophenyl-1*H*-1,2,3-triazole bromide **6** was prepared according to literature method [25].

*4.3. General Suzuki–Miyaura reaction procedure for cross-coupled product **8a-n**.*

1,4-dioxane (5 mL per 1 mmol) solution of **6** (1.0 equiv), K_3CO_3 (3.0 equiv per cross-coupling step), Pd $(PPh_3)_4$ (5 mol), and arylboronic acid **7a-n** (1.5 equiv per cross coupling step) was stirred at 120 ˚C for 8 h. After cooling to 20 ˚C, H_2O was added. The organic and the aqueous layers were separated, and the latter was extracted with CH_2Cl_2 (15 × 3 mL). The combined organic layer was dried over anhydrous Na_2SO_4, filtered, and the filtrate was concentrated in vacuo. The residue was purified by column chromatography (EtOAc/Hexane 9:1) to give a pure cross-coupled product **8a-n**.

(R)-4-(4-fluorophenyl)-1-(2-((3-methoxy-[1,1'-biphenyl]-4-yl)oxy)propyl)-1H-1,2,3-triazole ***(8a)****:*Colorless liquid; Yield = 76%; IR (liquid): 1494, 1216, 771, 743, 669 cm^{-1}; ^1H NMR (600 MHz, $CDCl_3$): δ 8.11 (1H, s), 7.77 (2H, dd, *J* = 6.0, 5.4 Hz), 7.49 (2H, d, *J* = 7.8 Hz), 7.39 (2H, t, *J* = 7.2 Hz), 7.30 (1H, t, *J* = 7.2 Hz), 7.07 (4H, dd, *J* = 8.4, 11.4 Hz), 6.88 (1H, d, *J* = 8.4 Hz), 4.72 (2H, m), 4.58 (1H, dd, *J* = 7.2 Hz), 3.84 (3H, s), 1.37 (3H, d, *J* = 6.6 Hz); ^{13}C NMR (150 MHz, $CDCl_3$): δ 163.4, 161.7,150.8, 146.7, 145.6, 140.7, 136.6, 128.7, 127.3, 127.1, 127.0, 126.9, 121.3, 119.6, 118.0, 115.8, 115.7, 111.3, 75.1, 55.7, 55.0, 17.3; ^{19}F NMR (564 MHz, $CDCl_3$): δ -113.89; HRMS (ESI^+): Found ($M+H^+$): 404.2002 $C_{24}H_{23}FN_3O_2$ required 404.2004.

(R)-4-(4-fluorophenyl)-1-(2-((3-methoxy-4'-methyl-[1,1'-biphenyl]-4-yl)oxy)propyl)-1H-1,2,3-triazole ***(8b)****:* Colorless liquid; Yield = 73%; IR (liquid): 1498, 1215, 750, 667 cm^{-1}; ^1H NMR (600 MHz, $CDCl_3$): δ 8.11 (1H, s), 7.77 (2H, dd, *J* = 5.4, 6.0 Hz), 7.39 (2H, d, *J* = 7.8 Hz), 7.21 (2H, t, *J* = 7.8 Hz), 7.08 (2H, t, *J* = 8.4 Hz), 7.04 (2H, t, *J* = 9.0 Hz), 6.86 (1H, d, *J* = 7.8 Hz), 4.71 (2H, m), 4.58 (1H, dd, *J* = 7.8 Hz), 3.83 (3H, s), 2.36 (3H, s), 1.36 (3H, d, *J* = 6.0 Hz); ^{13}C NMR (150 MHz, $CDCl_3$): δ 163.3, 161.7, 150.8, 146.7, 145.4, 137.8, 136.9, 136.6, 129.4, 127.3, 127.1, 126.7, 121.3, 119.3, 118.0, 115.8, 115.7, 111.1, 75.2, 55.7, 55.0, 21.0, 17.3; ^{19}F NMR (564 MHz, $CDCl_3$): δ -113.92; HRMS (ESI^+): Found ($M+H^+$): 418.2189 $C_{25}H_{25}FN_3O_2$ required 418.2186.

(R)-1-(2-((3,4'-dimethoxy-[1,1'-biphenyl]-4-yl)oxy)propyl)-4-(4-fluorophenyl)-1H-1,2,3-triazole ***(8c)****:* Yellow amorphous solid; Yield = 69%; IR (solid): 1497, 1237, 1215, 770, 744, 666 cm^{-1}; ^1H NMR (600 MHz, $CDCl_3$): δ 8.11 (1H, s), 7.77 (2H, dd, *J* = 5.4 Hz), 7.42 (2H, d, *J* = 9.0 Hz), 7.08 (2H, t, *J* = 8.4 Hz), 7.00 (2H, dd, *J* = 4.8, 1.8 Hz), 6.93 (2H, d, *J* = 8.4 Hz), 6.85 (1H, d, *J* = 7.8 Hz), 4.73 (2H, m), 4.57 (1H, dd, *J* = 7.2, 7.8 Hz), 3.83 (3H, s), 3.82 (3H, s), 1.36 (3H, d, *J* = 6.6 Hz); ^{13}C NMR (150 MHz, $CDCl_3$): δ 163.4, 161.7,159.0, 150.8, 146.7, 145.1, 136.3, 133.3, 127.9, 127.3, 121.3, 119.1, 118.2, 115.8, 115.6, 114.2, 111.0, 75.2, 55.7, 55.3, 55.0, 17.3; ^{19}F NMR (564 MHz, $CDCl_3$): δ -113.90; HRMS (ESI^+): Found ($M+H^+$): 434.1925 $C_{25}H_{25}FN_3O_3$ required 434.1927.

(R)-4-(4-fluorophenyl)-1-(2-((3-methoxy-4'-nitro-[1,1'-biphenyl]-4-yl)oxy)propyl)-1H-1,2,3-triazole ***(8d)****:* Yellow liquid; Yield = 85%; IR (liquid): 1597, 1496, 1345, 1217, 844, 772, 748, 668 cm^{-1}; ^1H NMR (600 MHz, $CDCl_3$): δ 8.24 (2H, d, *J* = 9.0 Hz), 8.08 (1H, s), 7.77 (2H, dd, *J* = 6.0, 5.4 Hz), 7.62 (2H, d, *J* = 8.4 Hz), 7.09 (4H, m), 6.91 (1H, d, *J* = 8.4 Hz), 4.74 (2H, m), 4.60 (1H, dd, *J* = 7.2 Hz), 3.87 (3H, s), 1.39 (3H, d, *J* = 6.6 Hz); ^{13}C NMR

(150 MHz, $CDCl_3$): δ 163.4, 161.8,150.9, 147.0, 146.8, 146.7, 133.6, 127.4, 127.3, 126.8, 124.1, 121.3, 120.1, 117.5, 115.9, 115.7, 111.2, 75.0, 55.9, 55.0, 17.3; ^{19}F NMR (564 MHz, $CDCl_3$): δ -113.52; HRMS (ESI^+): Found ($M+H^+$): 449.1811 $C_{24}H_{22}FN_4O_4$ required 449.1813.

*(R)-1-(2-((4'-chloro-3-methoxy-[1,1'-biphenyl]-4-yl)oxy)propyl)-4-(4-fluorophenyl)-1H-1,2,3-triazole (**8e**):* White solid; Yield = 82%; IR (solid): 1215, 770, 743, 668 cm^{-1}; ^1H NMR (600 MHz, $CDCl_3$): δ 8.10 (1H, s), 7.77 (2H, dd, *J* = 5.4 Hz), 7.41 (2H, d, *J* = 7.8 Hz), 7.35 (2H, d, *J* = 8.4 Hz), 7.08 (2H, t, *J* = 9.0 Hz), 7.00 (2H, t, *J* = 1.2 Hz), 6.87 (1H, d, *J* = 8.4 Hz), 4.72 (2H, m), 4.58 (1H, dd, *J* = 7.2 Hz), 3.84 (3H, s), 1.37 (3H, d, *J* = 6.6 Hz); ^{13}C NMR (150 MHz, $CDCl_3$): δ 163.4, 161.7, 150.8, 146.7, 145.9, 139.1, 135.2, 133.2, 128.8, 128.1, 127.3, 121.3, 119.4, 117.9, 115.8, 115.7, 111.0, 75.1, 55.8, 55.0, 17.3; ^{19}F NMR (564 MHz, $CDCl_3$): δ -113.81; HRMS (ESI^+): Found ($M+H^+$): 438.1292 $C_{24}H_{22}ClFN_3O_2$ required 438.1290.

*(R)-4'-((1-(4-(4-fluorophenyl)-1H-1,2,3-triazol-1-yl)propan-2-yl)oxy)-3'-methoxy-[1,1'-biphenyl]-4-carbonitrile (**8f**):* Pale yellow amorphous solid; Yield = 79%; IR (solid): 2225, 1496, 1215, 771, 744, 667 cm^{-1}; ^1H NMR (600 MHz, $CDCl_3$): δ 8.07 (1H, s), 7.76 (2H, dd, *J* = 6.0, 5.4 Hz), 7.66 (2H, d, *J* = 7.8 Hz), 7.57 (2H, d, *J* = 8.4 Hz), 7.06 (4H, m), 6.89 (1H, d, *J* = 8.4 Hz), 4.72 (2H, m), 4.58 (1H, dd, *J* = 7.2 Hz), 3.85 (3H, s), 1.38 (3H, d, *J* = 6.0 Hz); ^{13}C NMR (150 MHz, $CDCl_3$): δ 163.4, 161.7, 151.0, 146.8, 145.1, 134.1, 132.5, 127.4, 127.3, 121.2, 119.9, 118.8, 117.7, 115.8, 115.7, 111.21, 110.7, 75.0, 55.9, 55.0, 17.3; ^{19}F NMR (564 MHz, $CDCl_3$): δ -113.70; HRMS (ESI^+): Found ($M+H^+$): 429.1992 $C_{25}H_{22}FN_4O_2$ required 429.1995.

*(R)-1-(2-((4'-fluoro-3-methoxy-[1,1'-biphenyl]-4-yl)oxy)propyl)-4-(4-fluorophenyl)-1H-1,2,3-triazole (**8g**):* White solid; Yield = 84%; IR (solid): 1497, 1215, 771, 743, 668 cm^{-1}; ^1H NMR (600 MHz, $CDCl_3$): δ 8.10 (1H, s), 7.77 (2H, dd, *J* = 5.4 Hz), 7.43 (2H, dd, *J* = 5.4 Hz), 7.07 (4H, m), 6.99 (2H, d, *J* = 7.8 Hz), 6.86 (1H, d, *J* = 7.8 Hz), 4.71 (2H, m), 4.58 (1H, dd, *J* = 7.2 Hz), 3.84 (3H, s), 1.37 (3H, d, *J* = 6.0 Hz); ^{13}C NMR (150 MHz, $CDCl_3$): δ 163.4, 163.1, 161.7, 161.5, 150.8, 146.7, 145.6, 136.8, 135.6, 128.4, 127.3, 121.3, 119.4, 118.0, 115.8, 115.7, 115.6, 115.5, 111.1, 75.1, 55.8, 55.0, 17.3; ^{19}F NMR (564 MHz, $CDCl_3$): δ -113.82, -115.83; HRMS (ESI^+): Found ($M+H^+$): 422.1940 $C_{24}H_{22}F_2N_3O_2$ required 422.1938.

*(R)-4-(4-fluorophenyl)-1-(2-((3-methoxy-3',5'-bis(trifluoromethyl)-[1,1'-biphenyl]-4-yl)oxy)propyl)-1H-1,2,3-triazole (**8h**):* White amorphous solid; Yield = 80%; IR (solid): 1496, 1327, 1265, 1166, 1219, 772 cm^{-1}; ^{1}H NMR (600 MHz, $CDCl_3$): δ 8.07 (1H, s), 7.88 (2H, s), 7.79 (1H, s), 7.77 (2H, d, *J* = 5.4 Hz), 7.06 (3H, m), 7.02 (1H, s), 6.91 (1H, d, *J* = 7.8 Hz), 4.75 (2H, m), 4.59 (1H, dd, *J* = 7.2 Hz), 3.88 (3H, s), 1.39 (3H, d, *J* = 6.6 Hz); ^{13}C NMR (150 MHz, $CDCl_3$): δ 163.4, 161.8, 151.1, 147.0, 146.8, 142.8, 133.2, 132.0, 127.3, 127.2, 126.9, 124.2, 122.4, 121.2, 120.6, 120.0, 117.8, 115.8, 115.7, 111.2, 75.1, 56.0, 55.4, 17.2; ^{19}F NMR (564 MHz, $CDCl_3$): δ -62.81, -113.89; HRMS (ESI^+): Found ($M+H^+$): 540.1691 $C_{26}H_{21}F_7N_3O_2$ required 540.1693.

*(R)-4'-((1-(4-(4-fluorophenyl)-1H-1,2,3-triazol-1-yl)propan-2-yl)oxy)-3'-methoxy-[1,1'-biphenyl]-4-carbaldehyde (**8i**):* White amorphous solid; Yield = 77%; IR (solid): 1710, 1497, 1214, 743, 669 cm^{-1}; ^{1}H NMR (600 MHz, $CDCl_3$): δ 10.01 (1H, s), 8.10 (1H, s), 7.89 (2H, d, *J* = 7.8 Hz), 7.77 (2H, dd, *J* = 5.4 Hz), 7.64 (2H, d, *J* = 7.8 Hz), 7.09 (4H, m), 6.90 (1H, d, *J* = 7.8 Hz), 4.75 (2H, m), 4.59 (1H, dd, *J* = 7.2 Hz), 3.87 (3H, s), 1.39 (3H, d, *J* = 6.0 Hz); ^{13}C NMR (150 MHz, $CDCl_3$): δ 191.81, 163.4, 161.8, 150.9, 146.7, 146.6, 135.0, 134.7, 130.2, 127.4, 127.3, 126.8, 121.3, 120.0, 117.6, 115.8, 115.7, 111.2, 75.0, 55.9, 55.0, 17.3; ^{19}F NMR (564 MHz, $CDCl_3$): δ -113.54; HRMS (ESI^+): Found ($M+H^+$): 432.1761 $C_{25}H_{23}FN_3O_3$ required 432.1763.

*(R)-1-(2-((2',6'-difluoro-3-methoxy-[1,1'-biphenyl]-4-yl)oxy)propyl)-4-(4-fluorophenyl)-1H-1,2,3-triazole (**8j**):* Colorless liquid; Yield = 82%; IR (liquid): 1498, 1215, 754, 666 cm^{-1}; ^{1}H NMR (600 MHz, $CDCl_3$): δ 8.13 (1H, s), 7.78 (2H, dd, *J* = 5.4 Hz), 7.24 (1H, t, *J* = 7.2 Hz), 7.09 (2H, t, *J* = 8.4 Hz), 6.95 (4H, m), 6.89 (1H, d, *J* = 8.4 Hz), 4.73 (2H, m), 4.59 (1H, dd, *J* = 7.2 Hz), 3.80 (3H, s), 1.38 (3H, d, *J* = 6.0 Hz); ^{13}C NMR (150 MHz, $CDCl_3$): δ 163.5, 161.8, 160.9, 159.2, 150.2, 146.5, 146.0, 128.8, 128.7, 127.5, 127.4, 123.1, 121.5, 117.1, 115.9, 115.7, 114.4, 111.7, 111.6, 111.5, 74.8, 55.8, 55.1, 17.3; ^{19}F NMR (564 MHz, $CDCl_3$): δ -113.72, -114.33; HRMS (ESI^+): Found ($M+H^+$): 440.1896 $C_{24}H_{21}F_3N_3O_2$ required 440.1893.

*(R)-4-(4-fluorophenyl)-1-(2-((2',3',4'-trifluoro-3-methoxy-[1,1'-biphenyl]-4-yl)oxy)propyl)-1H-1,2,3-triazole (**8k**):* Colorless liquid; Yield = 86%; IR (liquid): 1499, 1215, 1068, 745, 669 cm^{-1}; ^{1}H NMR (600 MHz, $CDCl_3$): δ 8.09 (1H, s), 7.77 (2H, dd, *J* = 5.4 Hz), 7.08 (2H, t,

J = 8.4 Hz) 7.09 (3H, m), 6.95 (1H, d, *J* = 9.0 Hz), 6.88 (1H, d, *J* = 7.8 Hz), 4.73 (2H, m), 4.58 (1H, dd, *J* = 6.6, 7.2 Hz), 3.82 (3H, s), 1.38 (3H, d, *J* = 6.0 Hz); ^{13}C NMR (150 MHz, $CDCl_3$): δ 163.4, 161.7, 150.5, 146.8, 146.2, 128.8, 127.3, 127.0, 123.6, 123.5, 121.4, 121.3, 117.4, 115.8, 115.7, 112.9, 112.1, 112.0, 75.0, 55.8, 55.0, 17.3; ^{19}F NMR (564 MHz, $CDCl_3$): δ -113.79, -135.73, -138.72, -159.92; HRMS (ESI^+): Found ($M+H^+$): 458.1725 $C_{24}H_{20}F_4N_3O_2$ required 458.1723.

*(R)-4-(4-fluorophenyl)-1-(2-(2-methoxy-4-(naphthalen-2-yl)phenoxy)propyl)-1H-1,2,3-triazole (**8l**):* Pale brown amorphous solid; Yield = 79%; IR (solid): 1496, 1214, 743, 669 cm^{-1}; ^{1}H NMR (600 MHz, $CDCl_3$): δ 8.14 (1H, s), 7.93 (1H, s), 7.85 (3H, m), 7.79 (2H, dd, *J* = 5.4 Hz), 7.64 (1H, d, *J* = 8.4 Hz), 7.46 (2H, m), 7.18 (2H, d, *J* = 9.0 Hz), 7.09 (2H, t, *J* = 9.0 Hz), 6.92 (1H, d, *J* = 7.8 Hz), 4.73 (2H, m), 4.60 (1H, dd, *J* = 7.2, 6.6 Hz), 3.89 (3H, s), 1.39 (3H, d, *J* = 6.0 Hz); ^{13}C NMR (150 MHz, $CDCl_3$): δ 163.4, 161.8, 150.9, 145.7, 138.0, 136.5, 133.6, 132.5, 128.4, 128.0, 127.6, 127.4, 127.3, 126.9, 126.3, 125.9, 125.4, 125.3, 121.4, 119.9, 118.0, 115.8, 115.7, 111.4, 75.1, 55.8, 55.1, 17.3; ^{19}F NMR (564 MHz, $CDCl_3$): δ -113.74; HRMS (ESI^+): Found ($M+H^+$): 454.2133 $C_{28}H_{25}FN_3O_2$ required 454.2136.

*(R)-1-(4'-((1-(4-(4-fluorophenyl)-1H-1,2,3-triazol-1-yl)propan-2-yl)oxy)-3'-methoxy-[1,1'-biphenyl]-4-yl)ethanone (**8m**):* White solid; Yield = 82%; IR (solid): 1679, 1497, 1215, 841, 752, 670 cm^{-1}; ^{1}H NMR (600 MHz, $CDCl_3$): δ 8.09 (1H, s), 7.98 (2H, d, *J* = 8.4 Hz), 7.77 (2H, d, *J* = 5.4 Hz), 7.58 (2H, d, *J* = 8.4 Hz), 7.09 (4H, m), 6.89 (1H, d, *J* = 7.8 Hz), 4.73 (2H, m), 4.59 (1H, dd, *J* = 7.2 Hz), 3.86 (3H, s), 2.60 (3H, s), 1.38 (3H, d, *J* = 6.0 Hz); ^{13}C NMR (150 MHz, $CDCl_3$): δ 197.6, 163.4, 161.7, 150.9, 146.4, 145.2, 135.7, 134.9, 128.9, 127.3, 126.9, 121.3, 119.9, 117.7, 115.8, 115.7, 111.2, 75.1, 55.8, 55.0, 26.6, 17.3; ^{19}F NMR (564 MHz, $CDCl_3$): δ -113.77; HRMS (ESI^+): Found ($M+H^+$): 446.1645 $C_{26}H_{25}FN_3O_3$ required 446.1647.

*(R)-1-(2-(4-(benzo[b]thiophen-2-yl)-2-methoxyphenoxy)propyl)-4-(4-fluorophenyl)-1H-1,2,3-triazole (**8n**):* White amorphous solid; Yield = 78%; IR (solid): 1498, 1215, 1143, 1036, 747, 669 cm^{-1}; ^{1}H NMR (600 MHz, $CDCl_3$): δ 8.10 (1H, s), 7.78 (3H, m), 7.72 (1H, d, *J* = 7.8 Hz), 7.40 (1H, s), 7.32 (1H, t, *J* = 7.2 Hz), 7.28 (1H, t, *J* = 7.8 Hz), 7.18 (2H, m), 7.09 (2H, t, *J* = 8.4 Hz), 6.86 (1H, d, *J* = 8.4 Hz), 4.73 (2H, m), 4.58 (1H, dd, *J* = 7.2 Hz), 3.87 (3H, s), 1.37 (3H, d, *J* = 6.6 Hz); ^{13}C NMR (150 MHz, $CDCl_3$): δ 163.4, 161.8, 150.9,

146.7, 146.4, 143.7, 140.6, 139.3,129.6, 127.4, 127.3, 126.9, 124.5, 124.2, 123.4, 122.1, 121.3, 119.3, 119.0, 117.9, 115.8, 115.7, 110.6, 75.1, 55.8, 55.0, 17.2; ^{19}F NMR (564 MHz, $CDCl_3$): δ -113.74; HRMS (ESI^+): Found ($M+H^+$): 460.1686 $C_{26}H_{23}FN_3O_2S$ required 460.1684.

***In vitro* α-glucosidase inhibition assay**

α-Glucosidase inhibitory activity was evaluated by using 0.1 M phosphate buffer (pH 6.8) at 37 ˚C [32]. The enzyme (0.2 U/mL) in phosphate buffered saline was incubated with various concentrations of test compounds at 37 ˚C for 15 min. The substrate, *p*-nitrophenyl-*α*-D-glucopyranoside (0.7 mM, final) was then added and the change in absorbance at 400 nm was monitored for 30 min using a spectrophotometer (Spectra max M2, Molecular Devices, CA, USA). Test compound was replaced with DMSO-d_6 (7.5% final) in the control. Acarbose was used as the standard inhibitor. The percent inhibition was calculated by using the following formula:

$$\% \text{ Inhibition} = 100-(\text{OD test well}/\text{OD control}) \times 100$$

Molecular Modelling and Docking Studies

Docking was carried out using Molecular Operating Environment [41]. The 3D- structures of ligands were constructed on MOE, and wash module was used to add hydrogen and partial charges on ligands. Ligands were minimized with AMBER12:EHT force field until the gradient was reached to 0.1kcal/mol/A^2. For docking, homology modeling of *S. cerevisiae α*-glucosidase enzyme (UniprotKB accession number P53341) (https://www.uniprot.org/uniprot/P53341) was performed on SwissModel server (https://swissmodel.expasy.org/) by using 3A47 and 3AXH as templates. The stereochemical and geometrical properties of generated models were evaluated by Procheck [42], ERRAT (http://servicesn.mbi.ucla.edu/ERRAT/) and verify3D (http://servicesn.mbi.ucla.edu/Verify3D/). The best model was selected for further study. Hydrogen and partial charges were added on Protein file by Protonate3D command and minimize the structure with AMBER12:EHT force field. Water molecules in the active site, were included in protein during docking. Docking was carried out with Alpha Triangle placement method and London dG scoring function [41].

Conflict of interest

All authors confirm that this article content has no conflict of interest.

Acknowledgement

The authors would like to thank the University of Nizwa for the generous support of this project. We thank analytical and technical staff for assistance.

References

[1] B. F. A. Wahab, E. A. Latif, H. A. Mohamed, G. E. A. Awad, Design and synthesis of new 4-pyrazolin-3-yl-1,2,3-triazoles and 1,2,3-triazol-4-yl-pyrazolin-1-ylthiazoles as potential antimicrobial agents, Eur. J. Med. Chem. 52 (2012) 263-268.

[2] N. Singh, S. K. Pandey, R. P. Tripathi, Regioselective [3+2] cycloaddition of chalcones with a sugar azide: easy access to 1-(5-deoxy-D-xylofuranos-5-yl)-4,5-disubstituted-1*H*-1,2,3-triazoles, Carbohydr. Res. 354 (2010) 1641-1648.

[3] H. C. Kolb, K. B. Sharpless, The growing impact of click chemistry on drug discovery, Drug Discov. Today 8 (2003) 1128-1137.

[4] P. Thirumurugan, D. matosiuk, K. Jozwaik, Click Chemistry for Drug Development and Diverse Chemical–Biology Applications, Chem. Rev. 113 (2013) 4905-4979.

[5] M. J. Genin, D. A. Allwine, D. J. Anderson, M. R. Barbachyn, D. E. Emmert, S. A. Garmon, D. R. Graber, K. C. Grega, J. B. Hester, D. K. Hutchinson, Substituent Effects on the Antibacterial Activity of Nitrogen−Carbon-Linked (Azolylphenyl)oxazolidinones with Expanded Activity Against the Fastidious Gram-Negative Organisms *Haemophilus influenzae* and *Moraxella catarrhalis,* J. Med. Chem. 43 (2000) 953-970.

[6] R. Alvarez, S. Velazquez, A. San-Felix, S. Aquaro, E. D. Clercq, C.-F. Perno, A. Karlsson, J. Balzarini, M. J. Camarasa, 1,2,3-Triazole-[2,5-Bis-O-(tert-butyldimethylsilyl)-.beta.-D-ribofuranosyl]-3'-spiro-5"-(4"-amino-1",2"-oxathiole 2",2"-dioxide) (TSAO) Analogs: Synthesis and Anti-HIV-1 Activity, J. Med. Chem. 37 (1994) 4185-4194.

[7] S. Velazquez, R. Alvarez, C. Perez, F. Gago, E. De Clercq, J. Balzarini, M. Camarasa, Regiospecific synthesis and anti-human immuno-deficiency virus activity of novel 5-substituted N-alkylcarbamoyl and N,N-dialkyl carbamoyl 1,2,3-triazole-TSAO analogues, Antiviral Chem. Chemother. 9 (1998), 481-489.

[8] M. L. G. Ferreira, L. C. S. Pinheiro, O. A. Santos-Filho, M. D. S. Pecanha, C. Q. Sacramento, V. Machado, V. F. Ferreira, T. M. L. Souza, N. Boechat, Design, synthesis, and antiviral activity of new 1*H*-1,2,3-triazole nucleoside ribavirin analogs, Med. Chem. Res. 23 (2014) 1501-1511.

[9] D. R. Buckle, C. J. Rockell, H. Smith, B. A. Spicer, Studies on 1,2,3-triazoles. 13. (Piperazinylalkoxy)-[1]benzopyrano[2,3-d]-1,2,3-triazol-9(1H)-ones with combined H1-antihistamine and mast cell stabilizing properties, J. Med. Chem. 29 (1986) 2262-2267.

[10] C. Vicentini, V. Brandolini, M. Guarneri, P. Giori, Pyrazolo[3,4-d][1,2,3]triazole-1-carboxamides and 5-alkylaminopyrazolo[3,4-d]oxazoles: synthesis and evaluation of the in vitro antifungal activity, Farmaco (Societa chimica italiana: 1989) 47 (1992) 1021-1034.

[11] J. C. Fung-Tomc, E. Huczko, B. Minassian, D. P. Bonner, In Vitro Activity of a New Oral Triazole, BMS-207147 (ER-30346), Antimicrob. Agents Chemother. 42 (1998) 313-318.

[12] L. Dehestani, N. Ahangar, S. M. Hashemi, H. Irannejad, P. H. Masihi, A. Shakiba, S. Emami, Design, synthesis, in vivo and in silico evaluation of phenacyl triazole hydrazones as new anticonvulsant agents, Bio. Org. Chem. 78 (2018) 119-129.

[13] A. Stefanucci, W. Lei, S. Pieretti, E. Novellino, M.P. Dimmito, F. Marzoli, J.M. Streicher, and A. Mollica. On resin click-chemistry-mediated synthesis of novel enkephalin analogues with potent anti-nociceptive activity. Sci. Rep. 9 (2019) 5771.

[14] C. Peto, G. Batta, Z. Gyorgydeak, F. Sztaricskai, Glycoside Synthesis with Anomeric 1-*N*-Glycobiosyl-1,2,3-triazoles, J. Carbohydr. Chem. 15 (1996) 465-483.

[15] M. Kume, T. Kubota, Y. Kimura, H. Nakashmizu, K. Motokawa, M. Nakano, Orally Active Cephalosporins, J. Antibiot. 46 (1993) 177-182.

[16] K. Shalini, N. Kumar, S. Drabu, P. K. Sharma, Advances in synthetic approach to and antifungal activity of triazoles. Beilstein J. Org. Chem. 7 (2011) 668-677.

[17] I. K. Boddy, G. G. Briggs, R. P. Harrison, T. H. Jones, M. J. O'Mahony, I. D. Marilow, B. G. Roberts, R. J. Willis, R. Bardsley, J. Reid, The Synthesis and Insecticidal Activity of a Series of 2-Aryl-1,2,3-triazoles Pestic. M. Sci. 48 (1996) 189-196.

[18] X. Qin, H. B. Yu, H. Dai, Z. F. Qin, X. Zhang, G. F. Bing, T. T. Wang, J. X. Fang, Synthesis and plant-growth regulatory activities of novel imine derivatives containing 1*H*-1,2,4-triazole and thiazole rings, Chine. Chem. Lett. 21 (2010) 283-286.

[19] W. Q. Fan, A. R. Katritzky, in: A. R. Katritzky, C. W. Rees, E. F. V. Scriven (Eds.), *Comprehensive Heterocyclic Chemistry II*, Elsevier Science, Oxford, 4 (1996), 1-126.

[20] V. A. Motornov, A. A. Tabolin, R. A. Novikov, Y. V. Nelyubina, S. L. Loffe, I. V. Smolyar, V. G. Nenajdenko, Synthesis and Regioselective N-2 Functionalization of 4-Fluoro-5-aryl-1,2,3-N*H*-triazoles, Eur. J. Org. Chem. 46 (2017) 6851-6860.

[21] H. G. Bonacorso, M. C. Moraes, C. W. Wiethan, F. M. Luz, A. R. Meyer, N. Zanatta, M. A. P. Martins, Synthesis of 1*H*-1,2,3-triazoles—*Rufinamide* analogs by 1,3-dipolar cycloaddition and eletrocyclization reactions of trifluoroacetyl enolethers under thermal solventless conditions, J. Fluor. Chem. 156 (2013) 112-119.

[22] D. Wang, W. Sun, T. Chu, Synthesis of 5-Fluorotriazoles by Silver-Mediated Fluorination of 5-Iodotriazoles, Eur. J. Org. Chem. 19 (2015) 4114-4118.

[23] B. T. Worrell, J. E. Hein, V. V. Fokin, Angew. Chem. Int. Ed. 124 (2012) 11961-11964. Halogen Exchange (Halex) Reaction of 5-Iodo-1,2,3-triazoles: Synthesis and Applications of 5-Fluorotriazoles, Angew. Chem. Int. Ed. 51 (2012) 11791-11794.

[24] P. Zhang, M. G. Russell, T. F. Jamison, Continuous Flow Total Synthesis of Rufinamide, Org. Process Res. Dev. 18 (2014) 1567-1570.

[25] A. Mollica, G. Zengin, S. Durdagi, R. Ekhteiari Salmas, G. Macedonio, A. Stefanucci, M.P. Dimmito, and E. Novellino. Combinatorial peptide library screening for discovery of diverse α-glucosidase inhibitors using molecular dynamics simulations and binary QSAR models. J. Biomol. Struct. Dyn. 37 (2019) 726-740.

[26] M.C. Picot, G. Zengin, A. Mollica, A. Stefanucci, S. Carradori, and M. Mahomoodally. In vitro and in silico studies of mangiferin from Aphloia theiformis on key enzymes linked to diabetes type 2 and associated complications. Med. Chem. 13 (2017) 633-640.

[27] S. Shobana, Y. Sreerama, and N. Malleshi. Composition and enzyme inhibitory properties of finger millet (*Eleusine coracana* L.) seed coat phenolics: Mode of inhibition of α-glucosidase and pancreatic amylase. Food Chem. 115 (2009) 1268-1273.

[28] M.R. Bhandari, N. Jong-Anurakkun, G. Hong, and J. Kawabata. α-Glucosidase and α-amylase inhibitory activities of Nepalese medicinal herb Pakhanbhed (*Bergenia ciliata*, Haw.). Food Chem. 106 (2008) 247-252.

[29] G. Zengin, A. Stefanucci, M.J. Rodrigues, A. Mollica, L. Custodio, M.Z. Aumeeruddy, and M.F. Mahomoodally. *Scrophularia lucida* L. as a valuable source of bioactive compounds for pharmaceutical applications: In vitro antioxidant, anti-inflammatory, enzyme inhibitory properties, in silico studies, and HPLC profiles. J. Pharm. Biomed. Anal. 162 (2019) 225-233.

[30] A.D. Chougale, V.A. Ghadyale, S.N. Panaskar, and A.U. Arvindekar. Alpha glucosidase inhibition by stem extract of *Tinospora cordifolia*. J. Enzyme Inhib. Med. Chem. 24 (2009) 998-1001.

[31] G. Wang, Z. Peng, J. Wang, X. Li, J. Li, Synthesis, *in vitro* evaluation and molecular docking studies of novel triazine-triazole derivatives as potential α-glucosidase inhibitor, Eur. J. Med. Chem. 125 (2017) 423-429.

[32] S. K. Avula, A. Khan, N. Ur Rehman, M. U. Anwar, Z. Al-Abri, A. Wadood, M. Riaz, R. Csuk, A. Al-Harrasi, Synthesis of 1*H*-1,2,3-triazole derivatives as new *α*-glucosidase inhibitors and their molecular docking studies, Bioorg. Chem. 81 (2018) 98-106.

[33] N. Ur Rehman, A. Khan, A. Al-Harrasi, H. Hussain, A. Wadood, M. Riaz, Z. Al-Abri, New α-Glucosidase inhibitors from the resins of *Boswellia species* with structure–glucosidase activity and molecular docking studies, Bioorg. Chem. 79 (2018) 27-33.

[34] Z. Hassan, S. Al-Shdhani, A. Al-Ghafri, A. Al-Harrasi, J. Hussain, R. Csuk, Palladium-catalyzed chemo- and regioselective cross-coupling reactions of 2,3-dichloronaphthalene-1,4-bistriflate, Tetrahedron Lett. 52 (2015) 7141-7144.

[35] Z. Hassan, A. Al-Harrasi, T. Rizvi, J. Hussain, P. Langer, Selective Synthesis, Characterization of Isomerically Pure Arylated Benzo[1,2-*b*:6,5-*b*′]dithiophenes by Regioselective Suzuki–Miyaura Reaction and Evaluation of the Catalytic Properties of Nickel versus Palladium Complexes, Synthesis 49 (2017) 557-564.

[36] APEX, Bruker AXS, Madison, WI, USA.

[37] SAINT, Bruker AXS, Madison, WI, USA.

[38] SADABS, Bruker AXS, Madison, WI, USA.

[39] G. M. Sheldrick, *SHELXT* - Integrated space-group and crystal-structure determination, Acta Cryst. A71 (2015) 3-8.

[40] SHELXTL, Bruker AXS, Madison, Wisconsin, USA, 2015.

[41] Molecular Operating Environment, 2014. Chemical Computing Group ULC, 1010 Sherbooke St. West, Suite 910, Montreal, QC, Canada.

[42] R. A. Laskowski, M. W. MacArthur, D. S. Moss, J. M. Thornton, PROCHECK - a program to check the stereochemical quality of protein structures. J. App. Cryst. 26 (1993) 283-291.

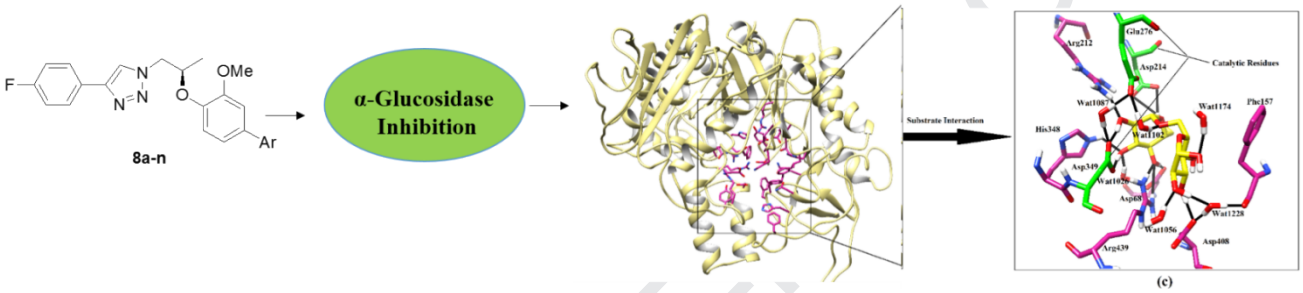

- A novel series of (*R*)-4-fluorophenyl-1*H*-1,2,3-triazole derivatives (**8a-n**) were synthesized.
- The structures were confirmed by ^{1}H NMR, ^{13}C NMR, ^{19}F NMR, ESI-MS, and single crystal X-ray diffraction.
- All compounds displayed significant α-glucosidase inhibition with IC_{50} values of 17.9 - 193.7 µM.
- Molecular docking studies were performed to establish their structure-activity relationship and binding interaction at atomic level.